Soils and Rocks
An International Journal of Geotechnical and Geoenvironmental Engineering
www.soilsandrocks.com
ISSN 1980-9743
ISSN-e 2675-5475

Energy measurement in a mechanized SPT equipment

Eduardo Oliveira Muguet[1,2#], Guilherme Alan Souza Costa[1,3], Flávia Sampaio Cabral[1,4], Fernando Artur Brasil Danziger[1,5]

Article

Keywords
SPT
Energy ratio
Mechanized SPT equipment
Automatic hammer
Drop height
Rod length effect

Abstract
This study presents the results of measurements performed during SPTs conducted with a mechanized system as part of the soil investigation for Paranaguá harbor, in Paraná state, Brazil. The energy delivered to the rod stem was measured in ninety-two blows. Additionally, the hammer and rod displacements were independently measured in thirty-one of these blows, which allowed the quantification of all energy losses, from the hammer release to the rod stem just below the anvil. The results showed that, for the particular equipment used, secondary impacts within the same blow have less influence on the energy transferred to the rod stem. This resulted in the energy ratio varying with depth, unlike in significant previous experience, where it was found to be constant.

1. Introduction

The SPT is an in situ test regularly used in several countries (Décourt et al., 1988) for onshore investigations and a broad range of geotechnical applications, such as the estimation of pile capacity (e.g., Aoki & Velloso, 1975; Décourt & Quaresma, 1978; Décourt, 1982), the assessment of friction angle in sands (e.g., Hatanaka & Uchida, 1996; Mayne, 2001), the assessment of geotechnical parameters of granitic saprolitic soils (e.g., Gomes Correia et al., 2004) and the evaluation of liquefaction resistance of sandy soils (e.g., Seed et al., 1985). Comprehensive state-of-the-art reports on SPT, including its main applications, were presented by Mello (1971) and Décourt (1989).

Different types of SPT equipment yield distinct *N*-values because energy losses may differ throughout all phases of the test, even when the potential energy input is the same across systems. Clayton (1990) considers that Palmer & Stuart (1957) were the first to suggest, which was shown later experimentally by Schmertmann & Palacios (1979), that *N*-value (at least for $N \leq 50$), varies inversely with the energy reaching the rod stem (Enthru energy) (Equation 1).

$$N_1 E_1 = N_2 E_2 \tag{1}$$

where N_1 and N_2 are *N*-values, and E_1 and E_2 are the corresponding energies reaching the rod stem (just below the anvil).

To properly compare *N*-values from different equipment, a standardization has been proposed, and it was established by the international standard ISO 22476-3 (ISO, 2005) that the *N*-value obtained in the test must be adjusted to a reference energy ratio of 60% (Equation 2).

$$N_{60} = \frac{E_R}{60} \cdot N \tag{2}$$

where N_{60} is the energy-corrected blow count; E_R is the equipment energy ratio, defined as the ratio of the energy actually reaching the rod stem, E_i, to the theoretical hammer energy (herein also named nominal energy), E^*. Under ISO (2005), the nominal energy is 473.4 J for a 63.5-kg hammer with a 760-mm drop height. The Brazilian standard (ABNT, 2020a) adopts 478.2 J (65-kg hammer, 750-mm drop), i.e., approximately 1% higher than the ISO (2005) value.

Mechanized SPT procedures were incorporated into the most recent Brazilian standard (ABNT, 2020a). The standard is divided into two parts: manual systems (hand-lifted and released pin-weight or donut hammers) and mechanized systems. Table 1 provides a cross-standard comparison and summarizes the mechanized-system requirements specified by the Brazilian standard.

#Corresponding author. E-mail address: eduardomuguet@gmail.com
[1]Universidade Federal do Rio de Janeiro, Instituto Alberto Luiz Coimbra de Pós-graduação e Pesquisa de Engenharia, Rio de Janeiro, RJ, Brasil.
[2]Logtest Instrumentações Geotécnicas, Rio de Janeiro, RJ, Brasil.
[3]Universidade Tecnológica Federal do Paraná, Coordenação de Engenharia Civil, Toledo, PR, Brasil.
[4]Redav Serviços de Engenharia, Rio de Janeiro, RJ, Brasil.
[5]Universidade Federal do Rio de Janeiro, Escola Politécnica, Rio de Janeiro, RJ, Brasil.

Submitted on September 6, 2025; Final Acceptance on February 3, 2026; Discussion open until November 30, 2026.
Editor: Renato P. Cunha https://orcid.org/0000-0002-2264-9711
https://doi.org/10.28927/SR.2026.004024

This is an Open Access article distributed under the terms of the Creative Commons Attribution license (https://creativecommons.org/licenses/by/4.0/), which permits unrestricted use, distribution, and reproduction in any medium, provided the original work is properly cited.

Table 1. Comparison of American, International and Brazilian Standards.

Test / Equipment Parameters	ASTM D1586-18 (ASTM, 2018)	ISO 22476-3 (ISO, 2005)	ABNT NBR 6484 (ABNT, 2020a) (mechanized system)
Hammer Shape	NS[a]	NS[a]	cylindrical shape
Hammer mass (kg)	63.5 ± 1	63.5 ± 0.5	65.0 ± 0.5
Drive assembly mass (kg)	NS[a]	< 115	NS[a]
Hammer/lift and release method	cathead, trip, automatic, semi-automatic, safety	automatic release mechanism	mechanized
Anvil specifications	NS[a]	NS[a]	Mass 7.5-8.5kg
Cushion	Not allowed	NS[a]	NS[a]
Drop Height (cm)	76 ±2.5	76 ±1.0	75 ±1.5
Blow Rate (blows/min)	NS[a,b]	NS[a]	10-40

[a]NS: Not specified. [b]It is highlighted that this rate depends on the type of equipment.

Given the diversity of equipment and techniques, it is essential to clarify the terms used herein. The hammer lifting and releasing systems of the SPT can be manual or mechanized, allowing any possible combination in practice.

The manual lifting system (hand lifting) consists of two workers lifting the hammer, which is attached to a rope that passes through a pulley at the top of the equipment tower. This lifting system can be associated with manual release (hand dropped), when the operators, upon identifying the specified height, simply release the rope, or with the release of the hammer by some mechanized system (mechanical release).

It is herein designated semi-mechanized lifting system the one which requires operators to lift the hammer but without the need to impose physical effort. In this case, widely employed in the United States, a cathead is used; the operator only needs to pull the rope to create enough friction for the cylinder, rotating at a constant speed, to lift the hammer. The release could be by loosening the rope, performed manually by the operator, or with a trigger system that can be manual or automatic. In the manual trigger system, an operator is needed to activate it (like the Argentinian system or the "Furnas type", Belincanta, 1998; Belincanta & Cintra, 1998; and Tombi, a Japanese system, Skempton, 1986), whereas the automatic trigger does not (Clayton, 1990).

The mechanized lifting system, on the other hand, uses a hydraulically operated mechanism, with the hammer releasing automatically when a rotating chain reaches its maximum point.

Regarding the hammer, there are four types: pin-weight, donut, safety and automatic type (the latter term is used in the literature without definition of the shape, referring only to the fact that it is lifted by a chain). The literature does not clearly establish whether these are the only types, and designations vary; the terms are frequently mistaken for the processes of lifting and releasing the hammer.

Table 2 presents the energy ratio E_R for different systems. A large variation in the energy ratio is observed in the table, indicating the need to measure the energy for each drive-weight assembly, as ISO 22476-3 (ISO, 2005) states.

Table 3 presents the average energy ratios for Brazilian data sets, mainly for the hand-dropped pin-weight hammer system. Compared with the data in Table 2, the range appears narrower, likely reflecting differences among SPT systems. Still, both tables report averages, and substantial variability in drop height and, consequently, in the energy delivered to the rod stem may occur. Table 3 also presents results from a test performed with an automatic hammer (CME) and an automatic trip hammer (donut-type, mechanically released). Although only five blows were measured, the CME hammer yielded the lowest energy ratio (41%). It is noteworthy that although the energy ratio was not measured directly, Hachich et al. (2006) presented evidence suggesting that the pin-weight hammer hand dropped system was more efficient than the CME hammer system.

Data from Table 3 indicate that the *N*-value obtained with a manual system (using a rope-and-pulley mechanism to lift and release the pin-weight hammer) should be multiplied by a factor between 1.2 and 1.5 to obtain N_{60}.

Although mechanized SPT systems currently account for most equipment worldwide, the hand lifted and released hammers - particularly pin-weight - remain common practice in Brazil and are also used in other countries (e.g., Yoshimi & Tokimatsu, 1983; Schnaid et al., 2009; Batilas et al., 2017; Ortiz et al., 2025). As mechanized SPT systems have been adopted in Brazil over the past few years and explicitly incorporated into the Brazilian standard (ABNT, 2020a), quantifying the energy delivered by mechanized equipment is essential for reliable energy normalization and result interpretation.

2. Energy measurement and transmission

2.1 General

The energy just below the anvil (E_i) may be evaluated using the so-called EFV method, as given in Equation 3.

$$E_i = \int F \cdot v \cdot dt \tag{3}$$

Table 2. Energy ratio for different SPT systems used worldwide.

Reference	Hammer	Lifting and releasing method	Energy ratio (E_R) (%)
Kovacs et al. (1981)	Safety	rope and cathead (manual)	34-83
	Donut	rope and cathead (manual)	31-65
Riggs et al. (1984)	Safety	rope and cathead (manual)	52-98
	Automatic (CME[b])	hydraulically powered chain lift	83-93
Kovacs & Salomone (1984)	Donut	rope and cathead (manual)	67
	Donut	rope and cathead (mechanical release)	80
Seed et al. (1985)[a]	Safety	rope and cathead (manual)	63-72
	Donut (Automatic trip)	rope and cathead (mechanical release)	76-90
Skempton (1986)	Safety	rope and cathead (manual)	55
Clayton (1990)	Donut (Automatic trip)	rope and cathead (mechanical release)	69-75
Batchelor et al. (1995)	Safety	rope and cathead (manual)	51
	Safety	spooling winch	23
	Automatic (CME)	hydraulically powered chain lift	69-81
Johnsen at al. (2001)	Automatic (CME)	hydraulically powered chain lift	55-83
	Safety	spooling winch	34-72
	Safety	rope and cathead (manual)	63-66
	Donut	rope and cathead (manual)	31-53
Sancio & Bray (2005)	Safety	rope and cathead (manual)	55-66
Biringen & Davie (2008)	Automatic (CME)	hydraulically powered chain lift	81.5
Kelley & Lens (2010)	Automatic (CME)	hydraulically powered chain lift	80-90
	Safety	rope and cathead (manual)	60-69
Reading et al. (2010)	Donut	rope and cathead (mechanical release)	43-81
	Automatic (CME)	hydraulically powered chain lift	53-89
Yee et al. (2013)	Donut (Automatic trip)	not reported	84-94
Honeycutt et al. (2014)	Automatic (CME)	hydraulically powered chain lift	83
Ji et al. (2023)	Donut	spooling winch	74-84
Ortiz et al. (2025)	Donut	rope and winch (manual)	43-68
	Automatic (donut shape)	not reported	82-87

[a]Compiled from literature. [b]CME – Central Mine Equipment.

Table 3. Average energy ratio obtained in Brazil.

Reference	Hammer	Lifting and releasing method	Average Energy ratio (E_R) (%)
Belincanta (1985)	Pin-weight	rope and pulley (manual)	72
Belincanta (1998), Belincanta & Cintra (1998)	Pin-weight	rope and pulley (manual)	71
	Pin-weight	steel wire rope and pulley (manual)	70
	Donut	rope and pulley (manual)	66
Cavalcante (2002), Cavalcante et al. (2004), Danziger et al. (2006); Danziger et al. (2008)	Pin-weight	rope and pulley (manual)	82
Odebrecht (2003), Odebrecht et al. (2005)	Pin-weight	rope and pulleys (manual)	76
Aoki et al. (2007)	Automatic (CME)	hydraulically powered chain lift	41
Cavalcante et al. (2011)	Pin-weight	rope and pulley (manual)	73
Santana (2015), Santana et al. (2014)	Pin-weight	rope and pulley (manual)	91
Lukiantchuki (2012), Lukiantchuki et al. (2017)	Pin-weight	rope and pulley (manual)	77-80[a]
	Donut (Automatic trip)	rope and cathead (mechanical release)	83-84[a]

[a]From two sites.

where F and v are the axial force and velocity, obtained from strain-gauge-based force transducers and accelerometers, respectively.

When only force measurements are available, the energy can alternatively be evaluated using the *F2* method, given by Equation 4 and discussed further below, where Z is the rod impedance.

$$E_i = \frac{1}{z}\int F^2 \cdot dt \tag{4}$$

As an alternative to direct measurements, the energy E_i can also be evaluated relative to the reference energy E^* by accounting for energy losses at different stages of the test. For this purpose, efficiency factors e_1, e_2 and e_3 (Décourt, 1989) may be used, as expressed in Equation 5. In addition, an alternative factor e_1^* may be defined (Santana et al., 2013) using the actual potential energy (based on the measured drop height) as the reference instead of the nominal energy E^*. The efficiency factors are computed using Equations 6 to 10.

$$E_i = e_1 \cdot e_2 \cdot e_3 \cdot E^* \tag{5}$$

$$e_1 = \frac{E_k}{E^*} \tag{6}$$

$$e_1^* = \frac{E_k}{E_p} \tag{7}$$

$$e_2 \cdot e_3 = \frac{E_i}{E_k} \tag{8}$$

$$e_1 \cdot e_2 \cdot e_3 = E_R = \frac{E_i}{E^*} \tag{9}$$

$$e_1^* \cdot e_2 \cdot e_3 = \frac{E_i}{E_p} \tag{10}$$

where e_1 relates the kinetic energy (E_k) just before the impact to the free fall energy considering the nominal energy (E^*) and e_1^* considering the measured potential energy (E_p) based on the actual drop height; e_2 is associated to the loss of energy due to the presence of the anvil (e.g., Skempton, 1986; Décourt, 1989) and e_3 is a rod-length factor that accounts for the separation between hammer and anvil in rods shorter than 10 m, caused by the upward-traveling stress wave (Palacios, 1977; Schmertmann & Palacios, 1979; Skempton, 1986). This last factor is still an issue, as discussed in the following section.

2.2 The length effect issue

Palacios (1977) and Schmertmann & Palacios (1979) addressed the issue of rod length in the transmission of the energy from the hammer to the rods. According to those authors, the energy would only be fully transmitted (disregarding prior losses) if the rod exceeded a critical minimum length. For rods shorter than this critical length, the compression wave generated by the hammer impact on the anvil is reflected from the bottom of the sampler as a tension wave (in almost all cases). This reflected tension wave would cause the separation between the hammer and the anvil, interrupting energy transmission at time $t = 2\ l/c$, where l is the rod length and c the propagation velocity of the wave in steel. Although energy could be transmitted through secondary impacts within the same blow, the authors considered that subsequent impacts would not significantly contribute to the overall energy transfer.

Based on this rationale, Palacios (1977) used the mathematical model of Fairhurst (1961) to calculate the theoretical maximum energy that could be transferred to the rods before the arrival of the tensile wave for various rod lengths. For typical safety hammer and A-type rod impedance, he proposed a theoretical maximum efficiency factor, η_l (equivalent to e_3), as a function of rod length. This relationship is plotted as the continuous line in Figure 1.

The η_l factor proposed by Palacios (1977) was first used as a correction factor by Kovacs et al. (1981) for energy measurements obtained with the *F2* method. Their procedure involved dividing the measured energy for a given rod length by its corresponding η_l value, thereby normalizing the result to an equivalent "infinite rod length" condition. This correction was later formalized in the ASTM D4633-86 (ASTM, 1986) standard as a length factor, *K2*, defined as $1/\eta_l$. However, this recommendation has been omitted from the newer version of ASTM D4633-16 (ASTM, 2016). Driven by the same core concept, other authors have proposed different correction factors; a compilation of these key studies is presented in Table 4.

The authors herein assume that all length factors presented in Table 4 were intended for SPT tests performed with A rods (occasionally for N-type rods, according to Seed et al., 1985).

As mentioned before, Décourt (1989) referred to the length factor as e_3 and argued that using very low values contradicts his practical experience. He cited Seed et al. (1985) and Skempton (1986), who recommended a lower bound of 0.75.

Some years later, the *F2* method was replaced by the *EFV* method, in which signals from both accelerometers and force transducers were used, allowing the energy to be measured for subsequent impacts within the same blow (Sy & Campanella, 1991; Cavalcante, 2002; Odebrecht, 2003; Daniel et al., 2005; Odebrecht et al., 2005; Danziger et al., 2006; Cavalcante et al., 2011).

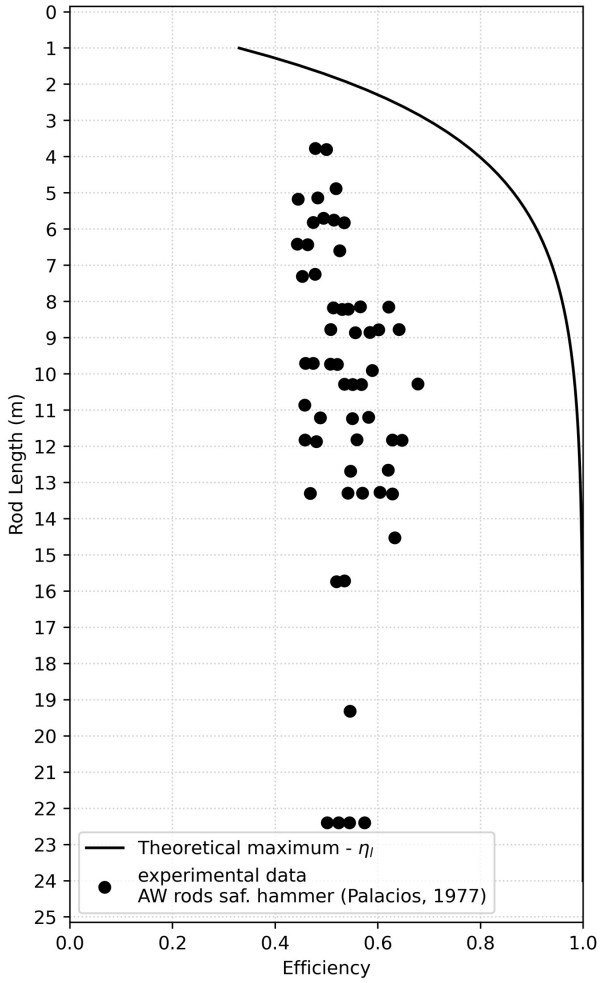


Figure 1. Rod length effect for a safety hammer with two-turn slip rope. Adapted from Schmertmann & Palacios (1979).

As an example, Figure 2 and 3 present results for a 2.39 m rod length for a pin-weight hammer hand lifted and released system. Figure 2 shows the initial loss-of-contact interval between the hammer and the rod. The energy delivered to the rod stem is shown in Figure 3. The data reveals that significant energy is transferred during subsequent impacts. When plotted against depth (Figure 4), the energy shows no depth dependence, indicating that rod length corrections are unnecessary for this data set. In other words, the subsequent impacts have been able to deliver to the rod stem the kinetic energy before the impact, reduced by the loss due to the anvil.

Similar conclusions and trends in the variation of energy with depth have been obtained by several authors (Sy & Campanella, 1991; Srithar & Ervin, 2001; Odebrecht, 2003; Daniel et al., 2005; Odebrecht et al., 2005), also indicating that no rod length correction should be used. Nevertheless, the rod length correction factor is included in ISO 22475-3 (ISO, 2005), as mentioned before. However, the standard ASTM D 4633-16 establishes:

> The correction for short rods of less than 30 ft (~9m), K2, was based on theoretical wave mechanics under the assumption that the hammer energy input was terminated by the reflective tensile wave and the remaining energy could be predicted. The factors never agreed with actual field measurements. Subsequent research has shown that this factor is not correct and should not be used. Liquefaction evaluation methods […] that advocate short rod correction factors based on the theoretical calculation are not correct (ASTM, 2016).

Furthermore, ASTM (2016) includes a note stating that "*Energy evaluation of the hammer system is more reliable when the length L is 9 to 12 m or more*", creating an internal inconsistency within this standard. This issue is further evidenced by the disagreement between ISO 22475-3 (ISO, 2005) – which was confirmed in 2024 by the responsible committee – and ASTM D4633 (ASTM, 2016), highlighting the lack of consensus on this subject.

Table 4. Rod-length correction factors from the literature.

Reference	Rod Length (m)				
	< 3	**3 to 4**	**4 to 6**	**6 to 10**	**> 10**
Seed et al. (1985)	0.75	1	1	1	1
Skempton (1986)	-	0.75	0.85	0.95	1
ASTM D4633 (ASTM, 1986)	0.69	0.69-0.76	0.76-0.89	0.89-0.98	0.98-1.00
Clayton (1990)	0.62	0.62-0.74	0.74-0.88	0.88-0.98	0.98-1.00
Morgano & Liang (1992)	0.86	0.86-0.90	0.90-0.96	0.96-0.99	1
Youd et al. (2001)	0.75	0.8	0.85	0.95	1
ISO 22475-3 (ISO, 2005)	-	0.75	0.85	0.95	1
ASTM D4633 (ASTM, 2016)	1	1	1	1	1

Adapted from Daniel et al. (2005), and updated by the authors.

CC BY

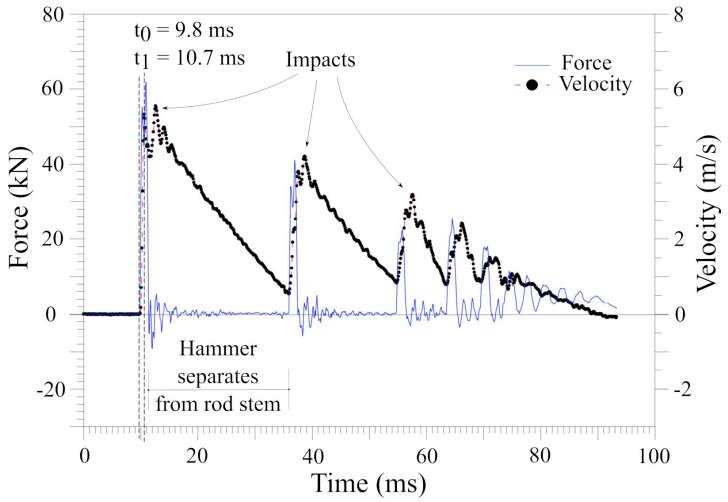


Figure 2. Force and velocity vs. time. Rod length = 2.39 m, N ≅ 2, sandy clay with gravel. Adapted from Cavalcante (2002), Cavalcante et al. (2004, 2011) and Danziger et al. (2006).

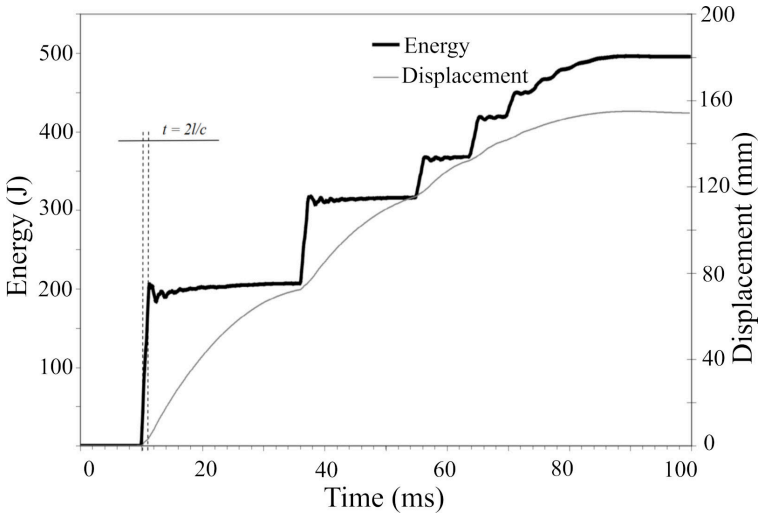


Figure 3. Energy and displacement vs. time. Rod length = 2.39 m, N ≅ 2, sandy clay with gravel. Adapted from Cavalcante (2002), Cavalcante et al. (2004, 2011) and Danziger et al. (2006).

3. Materials and methods

3.1 The equipment

This study utilized a Brazilian-manufactured mechanized SPT rig. The equipment features rubber caterpillar tracks and four hydraulic leveling pads. The SPT was performed using a 65 kg automatically released donut shape hammer. The hammer's enlarged top diameter allows it to be engaged by a wedge fixed to a hydraulically powered rotating chain. Once the hammer has been raised to 750 mm, the wedge releases it; it then free-falls along the guide rod (Figure 5). Rotary drilling is carried out with water circulation, and the borehole is cased with HW steel tubes.

Although lifting and releasing are automated, the hammer guide structure is hydraulically lowered after each blow, while the rotating chain lift mechanism simultaneously raises the hammer to the fixed 750 mm release point. This synchronized operation tries to restore the drop height without interrupting the cycle. For each blow, both the drop height and the blow-to-blow interval were recorded. Consequently, while the human factor is significantly reduced, it is not entirely eliminated from the SPT process.

Figure 6 shows the split anvil assembly, comprising an 11.7 kg upper part and a 3.2 kg lower part. The upper part is permanently fixed to the hammer guide and is secured within the rig tower by its shoulders (see Figure 5). The lower part is threaded onto the top drill rod. During testing, these parts mate via a concentric male–female interface, resting in

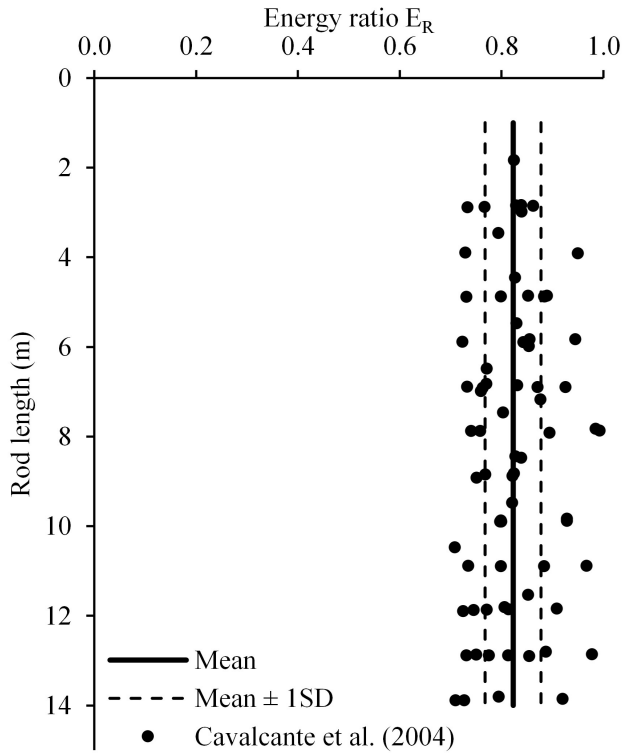


Figure 4. Energy ratio vs. rod length. Adapted from Cavalcante (2002), Cavalcante et al. (2004, 2011) and Danziger et al. (2006).

contact without fastening to form a single anvil for impact transmission. All tests employed AW rods and a standard Raymond-type split spoon sampler (51 mm outside diameter).

The equipment used in this study was manufactured prior to the publication of the updated Brazilian standard NBR 6484 (ABNT, 2020a). Consequently, its anvil mass and blow rate do not comply with the specifications of this subsequent standard.

3.2 The instrumentation

The energy immediately below the anvil was measured in a 50-cm-long instrumented rod equipped with strain gauges and accelerometers (5,000 g capacity). Data acquisition was performed with an SPT Analyzer at a sampling rate of 10 kHz. The instrumentation was calibrated in the laboratory prior to the field campaign. In addition to this widely used monitoring system, an independent setup was developed to track the displacements of the hammer and the top of the rod stem. Two linear potentiometers were mounted between a fixed frame on the rig and, respectively, the hammer and the upper rod. This system records signals for over 102 ms – exceeding the SPT Analyzer's acquisition window. Figure 7 illustrates the instrumentation used during a test, which records hammer and rod positions over time at 50,000 samples/s.

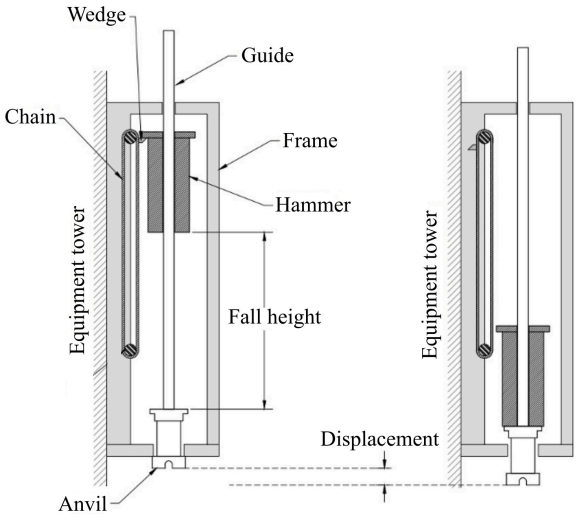


Figure 5. Hammer lifting-releasing system.



Figure 6. Two-part anvil assembly.

4. Tests performed and energy measurements

A geotechnical site investigation was conducted for the design of a harbor expansion in Paraná State, Brazil. The campaign included SPT and CPT, advancing to depths of 10 m and 16 m, respectively. Soil samples were retrieved from SPT at six depths for laboratory classification.

CC BY

The grain size analysis indicates that the soil profile to a depth of 10 m is predominantly composed of sand and gravel, with minor amounts of silt and clay. The SPTs in this study were performed at specific depths rather than at the standard 1-m intervals used in Brazilian practice, to accommodate the instrumentation setup for measuring energy transfer and hammer-rod displacements. A total of 92 blows from 9 tests (depths) were monitored with the SPT Analyzer, while hammer and rod displacements were specifically measured for 31 blows in 4 of these tests.

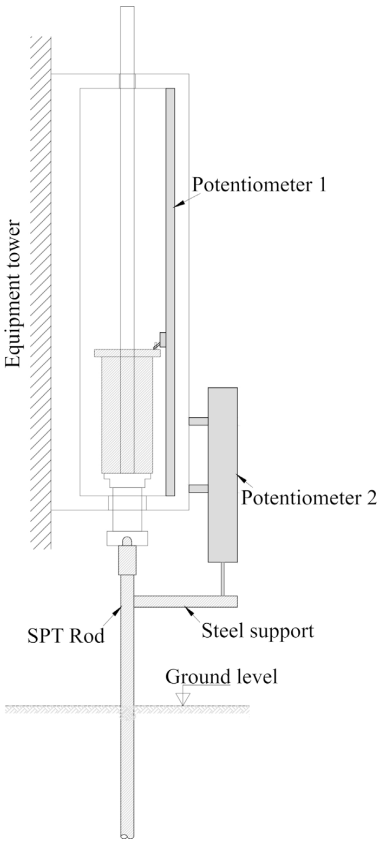


Figure 7. Potentiometer instrumentation setup.

Displacement–time records enable estimation of drop height and impact velocity. For each blow, the drop height equals the difference between the peak position and the position at impact. In the present study, impact velocity is computed by differentiating a smoothed displacement time-history curve and reading the value at impact.

This technique aligns with the methodology employed by Cavalcante et al. (2011) and Santana et al. (2013, 2014) in tests using a pin-weight hammer (hand lifted and released) system. In those studies, data acquisition relied on a high-speed camera, with results interpreted by analyzing the video frames. The underlying principle for determining impact velocity – differentiating the displacement time-history – is consistent with approaches reported in the literature (e.g., Cavalcante et al., 2011; Santana et al., 2013, 2014; Luza et al., 2024). While earlier studies obtained displacement data via high-speed video analysis, the present study uses potentiometers. To model the hammer displacement time-history, Cavalcante et al. (2011) approximated the drop curve with a fourth-degree polynomial function, whereas Santana et al. (2013, 2014) and Luza et al. (2024) found a second-degree function to be adequate.

In this study, the instrumentation collected approximately 4,000 samples per blow of the hammer motion, yielding a substantially higher displacement–time resolution than in the previously cited studies. Figure 8a presents the complete hammer displacement–time record, from which a drop height of 75.3 cm was measured. The figure also shows the first hammer–anvil impact and the final penetration, represented at the end of the curve by a displacement of 5.97 cm. Figure 8b provides a zoom-in view around the impact event. It can

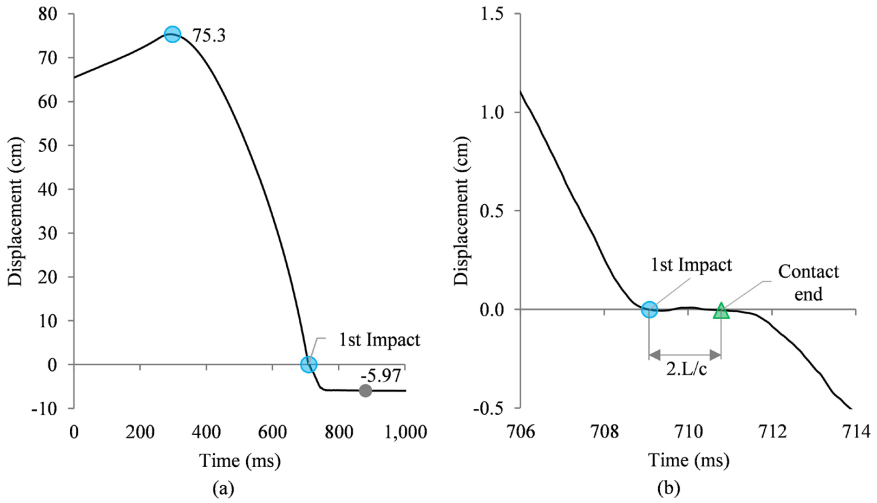


Figure 8. Hammer displacement–time record for the fourth blow at 2.3 m nominal depth (4.3 m long rod length) (a) full trace; (b) magnified view of the impact.

be observed that, for a short time interval of 1.71 ms, the hammer exhibits no measurable displacement; this interval is consistent with the theoretical value of 1.72 ms (corresponding to *2L/c*) for a rod length of 4.3 m.

The mean values of the measured and calculated parameters at each depth are included in Table 5. Energy just below the anvil (E_i) has been computed by Equation 3. Potential (E_p) and kinetic energy (E_k) have been computed according to Equations 11 and 12, respectively.

$$E_p = m \cdot g \cdot h_m \tag{11}$$

$$E_k = \frac{m \cdot v_{imp}^2}{2} \tag{12}$$

where m is the hammer mass, 65 kg, g is the gravitational acceleration, assumed as 9.81 m/s^2, h_m is the measured hammer drop height and v_{imp} is the measured impact velocity of the hammer. These last two values have been computed for each individual blow and the mean values are also presented in Table 5.

Table 5 presents the efficiency factors computed from Equations 6 to 10 for tests in which displacement measurements have been carried out. Because the measured energy E_i is influenced by both the anvil and the rod length, e_2 and e_3 cannot be separated directly from the data. Instead, their product $e_2.e_3$ was evaluated using Equation 8. The total efficiency was obtained from Equation 9 when the nominal potential energy was adopted, and from Equation 10 when the measured potential energy was used.

Figure 9 shows typical time histories of force and velocity for blow 2 at a nominal depth of 2.3 m (4.3-m rod stem). The same figure also presents the impact energy E_i at the rod stem, computed with the *EFV* method (Equation 3). The force and velocity traces highlight a dominant first impact followed by smaller secondary impacts that contribute little to the peak *EFV* energy. The *EFV* curve rises rapidly to about 250 J, indicating that, in this case, most of the energy is delivered during the initial contact.

5. Discussion

5.1 Drop height

Variability in drop height is a major drawback of the manually operated pin-weight hammer SPT system. A comprehensive study on this issue was conducted by Santana et al. (2014), who measured drop height in two deployments; data from one of them are reproduced in Figure 10, where a pronounced scatter is evident.

A different pattern was reported by Cavalcante et al. (2011), who measured drop heights within a much narrower range. In their tests, conducted by a very experienced operator, the mean drop height was 79 cm with a standard deviation of only 3 cm. The contrasting scatter observed in these SPT campaigns clearly shows how strongly drop height depends on the operator's experience and care, which in turn controls the variability of the energy delivered to the rod stem and, consequently, of the resulting *N*-values.

For comparison, Figure 10 includes the drop height measurements for the mechanized system, and Figure 11 presents the complete data set. In this case, all recorded drop heights lie between 74 cm and 78 cm.

Lukiantchuki (2012) and Lukiantchuki et al. (2017) monitored energy delivered by two different equipment setups: a hand-lifted and released pin-weight hammer and an automatic trip hammer. Although drop height was not monitored in their study (the authors reported that it was strictly controlled), the results indicated broadly similar performance for the two systems. The coefficient of variation of the energy ratio ($E_R = E_i/E^*$, Equation 9) was slightly higher for the manual system – 5.4% and 4.6% at the two sites – than for the automatic trip hammer, which yielded 5.2% and 3.7%, respectively. The corresponding energy ratio ranges for these tests are presented in Table 3.

Analysis of the 31 blows monitored revealed a very consistent mean drop height of 75.8 cm (SD = 1.0 cm; CV = 1.3%). This low scatter leads to a calculated mean potential energy that closely matches the nominal value of 478.24 J.

Table 5. Mean Measured and Calculated Quantities by Depth.

Nominal depth (m)	Rod lenght (m)	Blows	h_m (mm)	v_{imp} (m/s)	E_p (J)	E_k (J)	E_i (J)	e_1 E_k/E^*	e_1* E_k/E_p	$e_2.e_3$ E_i/E_k	e_1*.$e_2.e_3$ E_i/E_p	$e_1.e_2.e_3$ E_i/E^*
2.3	4.3	9	748	3.71	477.1	447.2	271.1	0.94	0.94	0.61	0.57	0.57
3.1	5.3	12	764	3.76	487.3	459.7	298.2	0.96	0.94	0.65	0.61	0.62
4.0	6.3	16	-	-	-	-	311.2	-	-	-	-	0.65
5.5	7.3	6	752	3.72	479.6	449.5	321.7	0.94	0.94	0.73	0.67	0.67
6.3	8.3	4	772	3.65	492.1	432.4	326.8	0.90	0.87	0.80	0.66	0.68
7.8	9.3	5	-	-	-	-	318.8	-	-	-	-	0.67
9.0	11.3	5	-	-	-	-	319.6	-	-	-	-	0.67
10.0	12.3	35	-	-	-	-	347.4	-	-	-	-	0.73

Legend: see List of symbols and abbreviations.

CC BY

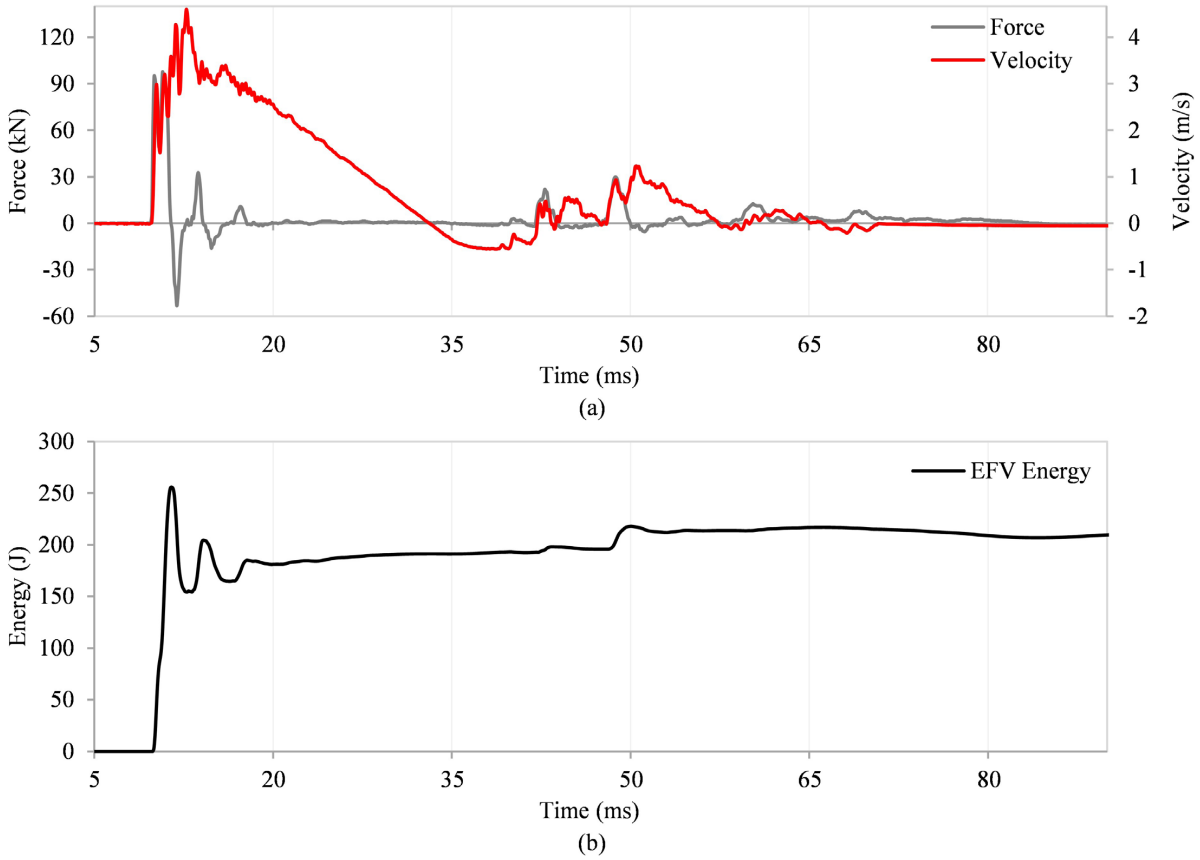


Figure 9. SPT Analyzer monitoring: (a) Force, and velocity vs. time; (b) Energy time-history measured just below the anvil (blow 2, 2.3 m depth, 4.3 m long rod stem).

Although the overall standard deviation lies within the ABNT (2020a) tolerance criteria (±1.5 cm, see Table 1), Figure 11 shows that a few individual measurements exceeded this limit.

During the initial tests with the mechanized SPT equipment, it became clear that the hammer blow rate (lifting-release frequency) influenced the drop height, as also reported by other authors (e.g., Kovacs, 1979; Farrar & Chitwood, 1999). Field observations indicated that, for the equipment used in this study, a blow rate of about 8 blows per minute was required to maintain a drop height of 75 cm.

Figure 12 shows the relationship between drop height and blow rate. Drop height was measured by the hammer potentiometer, and blow rate was determined from the timestamps recorded by the SPT Analyzer. For context, data from Borros AB (Kovacs, 1979) and CME (Farrar & Chitwood, 1999) automatic hammers are also included. All data sets consistently show a trend of increasing drop height with increasing blow rate. Although the blow rate remained within a narrow measured range, the data still show an increase in drop height with blow rate (Figure 12), consistent with prior reports for automatic systems. Therefore, controlling the blow rate is essential for reliable SPT results, even when using automated systems.

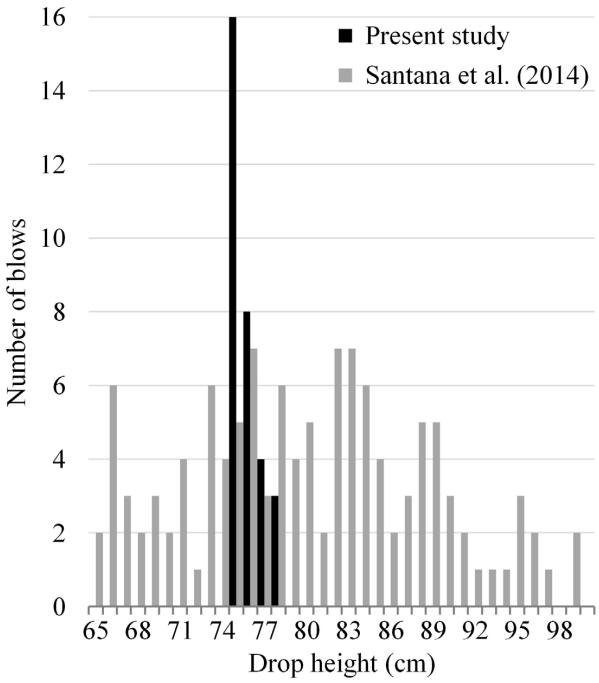


Figure 10. Hammer drop height measured in SPT. Adapted from Santana et al. (2014).

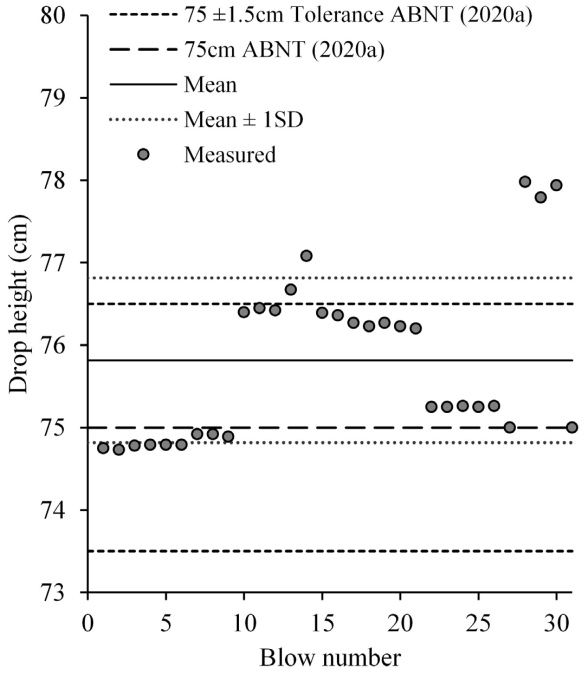


Figure 11. Measured drop height.

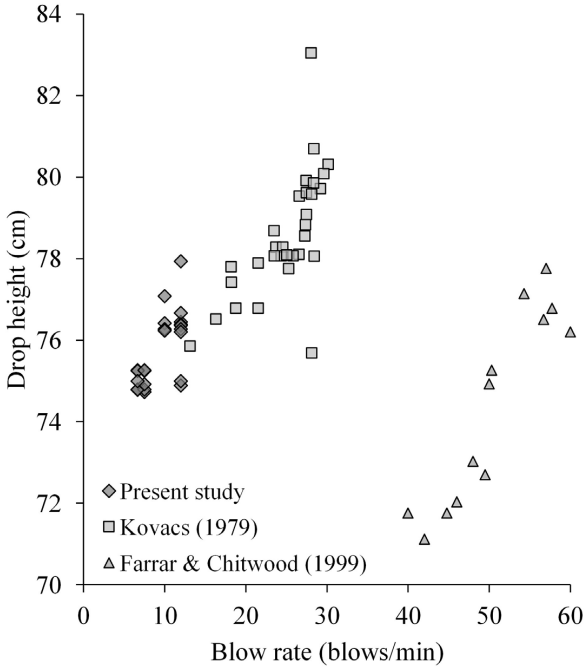


Figure 12. Influence of blow rate on hammer drop height.

5.2 Impact velocity

The mean measured hammer impact velocity was 3.73 m/s, representing a slight reduction of only 2.8% relative to the theoretical free-fall velocity (3.84 m/s) for a drop height of 75 cm. This minor loss indicates that friction in the mechanized release system was relatively limited under the test conditions. The mean impact velocities obtained at each depth from the potentiometer measurements are summarized in Table 5.

The efficiency factor e_1^*, which relates the kinetic energy at impact to the corresponding potential energy (Equation 7), was evaluated and is reported in Table 6. For comparison, Table 6 also includes data from Cavalcante et al. (2011) and Santana et al. (2014) for pin-weight hand-lifted systems. In the present study, e_1^* ranges from 0.87 to 0.99, with a mean value of 0.94. These values are close to those reported by Santana et al. (2014) and are higher than those measured by Cavalcante et al. (2011).

When the nominal potential energy is considered, the resulting energy ratio e_1 ranges from 0.90 to 1.00, with a mean value of 0.95.

5.3 Energy measured vs. rod length (depth)

The measured energies (E_i, E_K and E_P) and the energy ratio E_R, as functions of rod length, are shown in Figure 13. The potential and kinetic energies exhibit low variability, with coefficients of variation of 1.3% for E_P and 2.2% for E_K, consistent with the nearly constant input energy expected from an automated system. In contrast, E_i shows a clear increasing trend with rod length up to 7.3 m. Expressed in non-dimensional form, the energy ratio E_R ranges from 0.51 (4.3-m rod length) to 0.76 (12.3-m rod length), with an overall mean of 0.67 (67%); for the shortest rods, this means that the energy delivered to the rod stem can be roughly half of the nominal potential energy.

This range is lower than the typical energy-ratio interval of 71–91% previously reported in Brazilian studies for hand-lifted and released pin-weight hammers (Table 3). Consequently, for comparable soil conditions, the mechanized equipment investigated in this study is expected to produce higher *N*-values than traditional hand-lifted pin-weight hammers. If the analysis is restricted to tests with rod lengths greater than 7.3 m (where rod-length effects are expected to be negligible), the mean energy ratio is 71% when calculated from the entire data set. The average of the mean values across all individual tests in this range is 69%.

Table 6. Efficiency factor e_1^*.

Reference	Minimum	Mean	Maximum
Present study	0.87	0.94	0.99
Santana et al. (2014)	0.86	0.92	0.99
Cavalcante et al. (2011)	0.68	0.70	0.72

CC BY

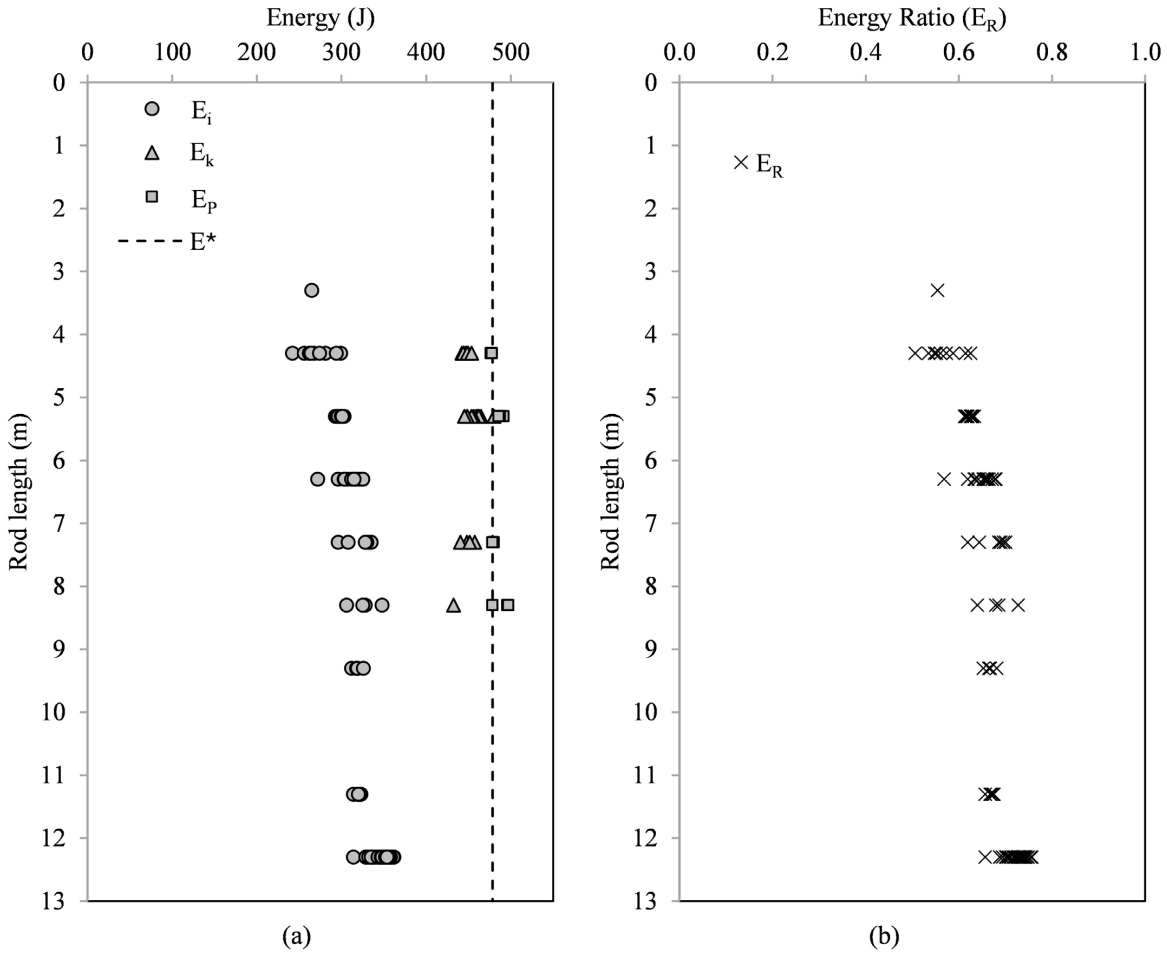


Figure 13. Measured energies and energy ratio: (a) Energies E_i, E_k, E_p; (b) Energy ratio E_R vs. rod length.

This systematic increase of energy with rod length appears to be a system-dependent feature of this particular mechanized SPT system. This underscores the need to measure the delivered energy for each system and to issue a certificate, as required by ISO (2005) and ABNT (2020b). It also highlights the value of profiling energy with depth when shallow-depth *N*-values are of particular interest.

5.4 Energy losses in the anvil

The energy E_i measured just below the anvil already accounts for the losses associated with the anvil (e_2) and with rod-length effects (e_3). Therefore, these two factors cannot be separated directly from the measurements. To do so, it is assumed that e_2 is independent of rod length. In addition, the measured values indicate that, for rod lengths equal to or greater than 7.3 m (Table 5), the length-effect factor can be taken as $e_3 = 1$, i.e., no significant rod-length effect is observed in this range. Kinetic energy was measured at four depths, corresponding to rod lengths of 4.3, 5.3, 7.3 and 8.3 m. Since rod-length effects are considered negligible around 7.3 m and 8.3 m rods ($e_3 = 1$), these two cases can be used to back-calculate e_2 (see Equation 9). For the 7.3 m rod, $e_1 = 0.94$, $e_3 = 1.0$ and $e_1.e_2.e_3 = 0.67$, which gives $e_2 = 0.71$. For the 8.3 m rod, $e_1 = 0.90$, $e_3 = 1.0$ and $e_1.e_2.e_3 = 0.68$, which gives $e_2 = 0.76$.

These values are lower than those reported for previous Brazilian experience, corresponding to lighter anvils (Décourt, 1989; Cavalcante et al., 2011; Santana et al., 2014), and lie near the upper bound suggested by Skempton (1986), as indicated in Figure 14.

5.5 Secondary impacts

Because previous studies have shown that secondary impacts can deliver additional energy to make the energy ratio effectively depth-independent ($e_3 \approx 1$) (e.g., Srithar & Ervin, 2001; Cavalcante, 2002; Odebrecht, 2003; Cavalcante et al., 2004, 2011; Daniel et al., 2005; Odebrecht et al., 2005; Lukiantchuki et al., 2017), the role of secondary impacts was examined for the mechanized system tested in this study. Independent measurement of hammer and rod displacements is particularly useful for this analysis. Figures 15 and 16, for rod lengths of 4.3 m and 7.3 m, respectively, illustrate the contribution of secondary impacts.

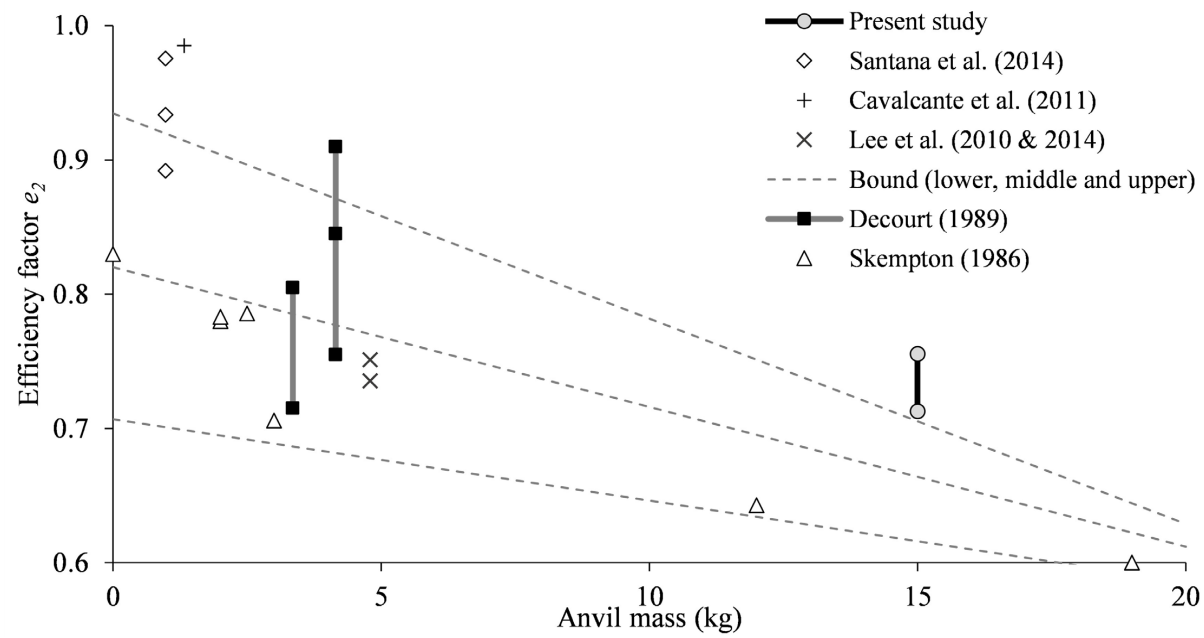


Figure 14. Efficiency factor e_2 as a function of anvil mass. Adapted from Décourt (1989), Cavalcante et al. (2011) and Santana et al. (2014).

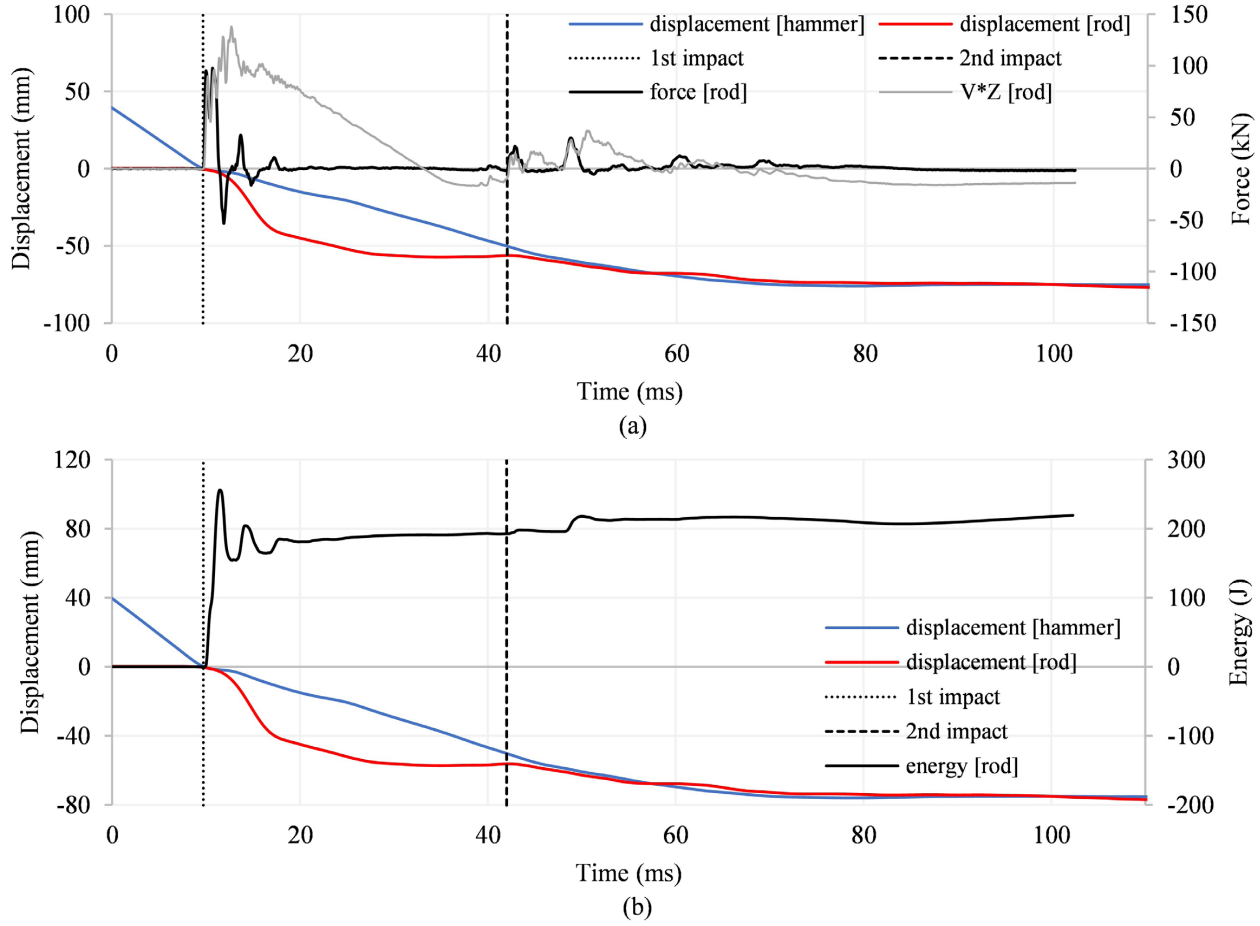


Figure 15. Secondary impact time-history: (a) force, velocity*Z and displacement (hammer and rods); (b) energy and displacement (hammer and rods). Rod length = 4.3 m, $N \cong 4$.

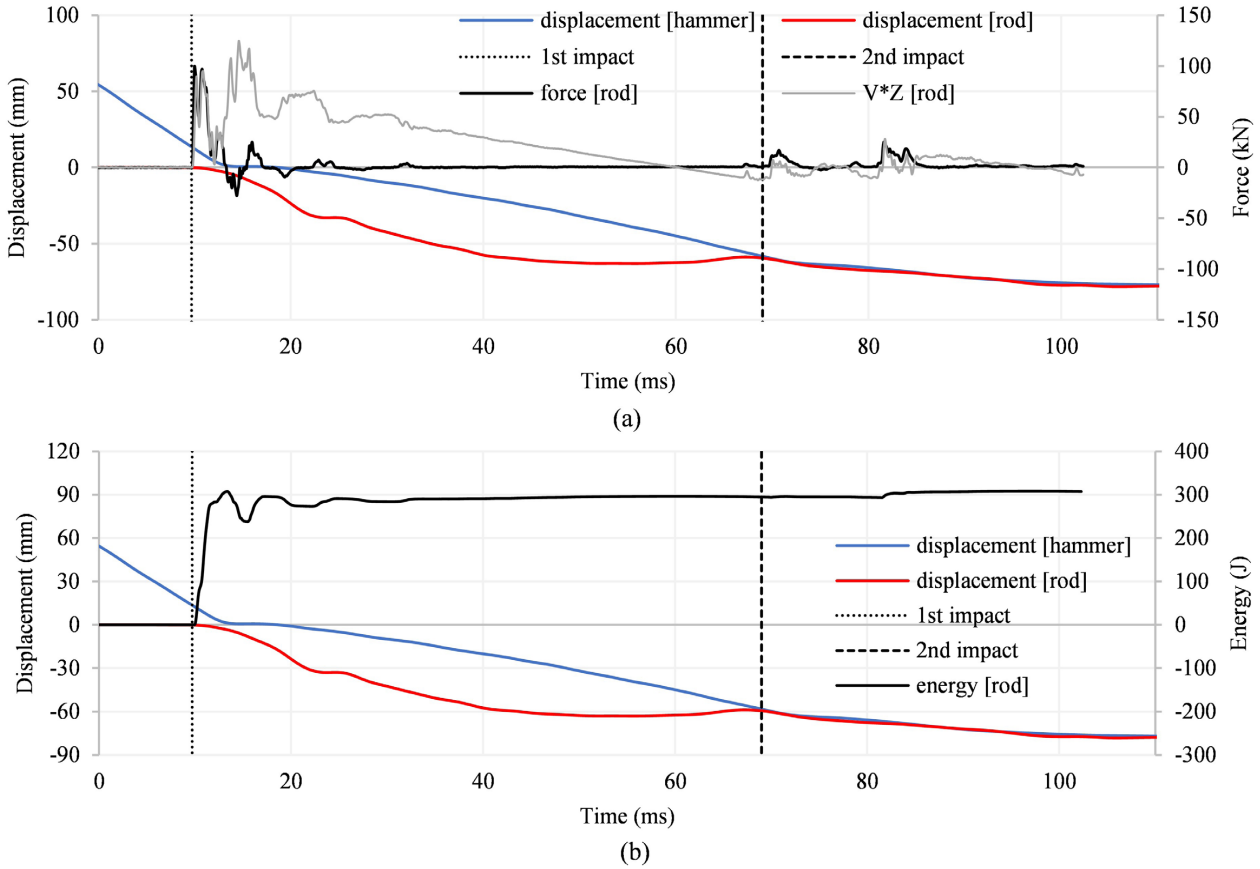


Figure 16. Secondary impact time-history: (a) force, velocity*Z and displacement (hammer and rods); (b) energy and displacement (hammer and rods). Rod length = 7.3 m, $N \cong 4$.

Independent measurements of hammer and rod displacements make it possible to identify two distinct hammer-rod contact events, regardless of rod length. These events are marked by the vertically dashed lines in Figures 15 and 16. The first impact is defined by a sudden increase in force at the rod (assumed greater than 1kN). The second impact is defined as the instant when the hammer and rod displacement time histories meet again after the first impact, i.e., when the hammer, having temporarily separated from the rod, catches up and recontacts it. As the rod length increases, the time interval between these two impacts increases, as expected from one-dimensional wave-propagation theory.

For the mechanized system herein studied, the hammer–rod contact history consistently exhibited two contacts per blow, but the second impact contributes negligible additional energy to the rods in the cases examined (Figures 15 and 16). In all blows analyzed, the EFV energy curve rises rapidly during the first impact and shows only a small increase associated with the second contact. This behavior contrasts with several studies on hand-lifted or safety hammers, where secondary impacts have been shown to transfer a significant portion of the energy and to produce nearly depth-independent energy ratios ($e_3 = 1$) (e.g., Srithar & Ervin, 2001; Cavalcante, 2002; Odebrecht, 2003; Cavalcante et al., 2004, 2011; Daniel et al., 2005; Odebrecht et al., 2005; Lukiantchuki et al., 2017; see also Figures 2 and 3). In the present mechanized system, secondary impact primarily increases the permanent displacement, as shown in Figures 15 and 16 by comparing the displacement at the second impact with the final displacement.

These observations reinforce that rod length effects and the role of secondary impacts can be system-dependent. Consistent with this view, Daniel et al. (2005) and Cetin et al. (2023) showed that short-rod correction factors are not universal, but may vary with rod length, *N*-value, and hammer-anvil configuration. In addition, our findings agree qualitatively with the detailed hammer-anvil motion studies of Lee et al. (2010, 2014). Using high-speed imaging and an instrumented rod to measure force and velocity, they demonstrated that the contribution of secondary impacts to both transferred energy and sampler penetration depends on the *N*-value and rod length and can be limited for certain equipment configurations.

6. Summary, conclusions and further remarks

Energy measurements were conducted during SPTs performed with a mechanized SPT equipment and AW rods, as

part of soil investigations for Paranaguá harbor, Paraná state, Brazil. The average energy ratio across all measured blows was 67%. When only rods longer than 7.3 m were considered, the average energy ratio increased to 71%. The energy ratio was found to vary with depth, unlike previous experience, which is attributed to the small influence of secondary impacts within the same blow on the energy transferred to the rod stem. Further research is needed on this particular issue, which remains controversial in international standards.

If the average energy ratio for the Brazilian hand-lifted and released equipment is in the range 72–84%, the *N*-value obtained with the mechanized system evaluated in this study is greater than that obtained with the hand-lifted and released equipment. In other words, using the *N*-value from this specific mechanized equipment, herein studied without proper consideration of the energy ratio, would lead to a foundation design on the unsafe side in the context of Brazilian engineering practice. This observation holds not only to the average energy ratio but also to cases where the energy ratio varies with depth. It is important to emphasize, however, that this conclusion applies only to the equipment tested herein, since other mechanized SPT systems reported in the literature have shown higher efficiencies, in the range of 80–90%.

The independent measurement of displacement of hammer and rod stem allowed the assessment of the efficiency factors e_1, in the range 0.90-0.96 and e_2, in the range 0.71-0.76.

A very small scatter for the drop height was obtained, provided that the blow rate was in the range of 8 blows/minute. As observed with other equipment, higher blow rates were associated with greater drop heights. This implies that, even for mechanized equipment, monitoring the blow rate to maintain the correct drop height remains necessary.

Acknowledgments

The authors would like to acknowledge the engineer Pedro Vieira from MTS Sistemas do Brasil for providing the accelerometers calibration.

Declaration of interest

The authors have no conflicts of interest to declare. All co-authors have observed and affirmed the contents of the paper and there is no financial interest to report.

Authors' contributions

Eduardo Oliveira Muguet: conceptualization, data curation, formal analysis, funding acquisition, investigation, methodology, project administration, software, visualization, writing – original draft, writing – review and editing. Guilherme Alan Souza Costa: conceptualization, data curation, formal analysis, visualization, writing – original draft, writing – review and editing. Flávia Sampaio Cabral: formal analysis, funding acquisition, visualization, writing – original draft. Fernando Artur Brasil Danziger: conceptualization, resources, supervision, validation, writing – review and editing.

Data availability

The data sets generated analyzed in the course of the current study are available from the corresponding author upon request.

Declaration of use of generative artificial intelligence

This work was prepared with the assistance of generative artificial intelligence (GenAI) tools, specifically Grammarly, with the aim of improving the text's coherence, ensuring a clear and logical flow. The entire process of using this tool was supervised, reviewed and always edited by the authors. The authors assume full responsibility for the content of the publication that involved the aid of GenAI.

List of symbols and abbreviations

e_1	Efficiency factor related to losses on hammer fall (based on nominal fall height)
e^*_1	Efficiency factor related to losses on hammer fall (based on measured fall height)
e_2	Efficiency factor ratio related to anvil energy losses
e_3	Efficiency factor ratio related to rod lengths
g	Gravitational acceleration
h_m	Measured drop height of the hammer
m	Mass of the hammer
t	Elapsed time since hammer release
v	Particle velocity on the instrumented rod, evaluated by acceleration signal
v_{imp}	Hammer impact velocity
AW	Rod stem (parallel-thread): 44.45 mm outside diameter; 7.6 cm^2 steel cross-section
CME	Central Mine Equipment
CPT	Cone penetration test
CV	Coefficient of variation
EF2	Energy on rod stem computed by recording force integration alone until $F = 0$
EFV	Energy on rod stem computed with force and velocity at the instrumented rod section
E_i	Energy reaching the rod stem
E^*	Nominal potential energy (also called theoretical potential energy)
E_k	Hammer kinetic energy just before impact
E_p	Hammer potential energy from measured drop height
E_R	Energy ratio
F	Measured force at the instrumented rod section
HW	Rod stem with 101 mm internal diameter used to case the drilling hole
N	Blow count

CC BY

N_{60}	Corrected blow count for a 60% efficiency
R^2	Coefficient of determination
SD	Standard deviation
SPT	Standard Penetration Test
Z	impedance
η_l	Efficiency factor related to rod lengths

References

ABNT NBR 6484. (2020a). *Soil: standard test method for standard penetration test.* ABNT – Associação Brasileira de Normas Técnicas, Rio de Janeiro, RJ (in Portuguese).

ABNT NBR 16796. (2020b). *Soil: standard method for energy evaluation in SPT.* ABNT – Associação Brasileira de Normas Técnicas, Rio de Janeiro, RJ (in Portuguese).

Aoki, N., & Velloso, D.A. (1975). An approximate method to estimate the bearing capacity of piles. In *Proceedings of the 5th. Panamerican Conf. of Soil Mechanics and Foundation Engineering* (Vol. 1, pp. 367-376), Buenos Aires. International Society of Soil Mechanics and Geotechnical Engineering.

Aoki, N., Esquivel, E.R., Neves, L.F.S., & Cintra, J.C.A. (2007). The impact efficiency obtained from static load test performed on the SPT sampler. *Soil and Foundation*, 47(6), 1045-1052. https://doi.org/10.3208/sandf.47.1045

ASTM D4633-86. (1986). *Standard test method for energy measurement for dynamic penetrometers*. ASTM International, West Conshohocken, PA.

ASTM D4633-16. (2016). *Standard test method for energy measurement for dynamic penetrometers*. ASTM International, West Conshohocken, PA. https://doi.org/10.1520/D4633-16.

ASTM D1586-18. (2018). *Standard test method for standard penetration test (SPT) and split-barrel sampling of soils.* ASTM International, West Conshohocken, PA. https://doi.org/10.1520/D1586_D1586M-18.

Batchelor, C., Goble, G.G., Berger, J., & Robert, M. (1995). Standard penetration test energy measurements on the Seattle ASCE Field Testing Program. In *Proceedings of the Seminar In situ Testing for Seismic Evaluation.* Goble Rausche Likins and Associates, Inc.

Batilas, A.V., Pelekis, P.C., Roussos, P.G., & Athanasopoulos, G.A. (2017). SPT energy measurements: manual vs. automatic hammer release. *Geotechnical and Geological Engineering*, 35(2), 879-888. https://doi.org/10.1007/s10706-016-0138-z.

Belincanta, A. (1985). *Dynamic energy in SPT: results from a theoretical-experimental investigation* [Master's dissertation]. University of São Paulo (in Portuguese).

Belincanta, A. (1998). *Evaluation of intervenient factors in the penetration resistance of the SPT* [Doctoral thesis]. University of São Paulo (in Portuguese).

Belincanta, A., & Cintra, J.C.A. (1998). Evaluation of intervenient factors on the ABNT method to SPT execution. *Solos e Rochas*, 21(3), 119-133.

Biringen, E., & Davie, J. (2008). Assessment of energy transfer ratio in SPT using automatic hammers. In *Proceedings of the GeoCongress 2008: Characterization, Monitoring, and Modeling of GeoSystems* (pp. 356-363), New Orleans, Louisiana.. https://doi.org/10.1061/40972(311)45.

Cavalcante, E.H. (2002). *Theoretical-experimental investigation of SPT* [Doctoral thesis]. COPPE, Federal University of Rio de Janeiro (in Portuguese).

Cavalcante, E.H., Danziger, B.R., & Danziger, F.A.B. (2011). Measurement of drop height and impact velocity in the Brazilian SPT system. *Soils and Rocks*, 34(3), 207-218. https://doi.org/10.28927/SR.343207.

Cavalcante, E.H., Danziger, F.A.B., & Danziger, B.R. (2004). Estimating the SPT penetration resistance from rod penetration based on instrumentation. In *Proceedings of the 2nd International Conference on Site Characterization* (Vol. 1, pp. 293-298). The Netherlands: Millpress.

Cetin, K.O., Cevik, M.E., Al-Suhaily, A., & Yunatci, A.A. (2023). Probabilistic assessment of standard penetration test hammer energy efficiency and rod length corrections. *Journal of Geotechnical and Geoenvironmental Engineering*, 149(8), 04023055. https://doi.org/10.1061/JGGEFK.GTENG-11136.

Clayton, C. (1990). SPT energy transmission: theory, measurement and significance. *Ground Engineering*, 23, 35-43.

Daniel, C.R., Howie, J.A., Jackson, R.S., & Walker, B. (2005). Review of standard penetration test short rod corrections. *Journal of Geotechnical and Geoenvironmental Engineering*, 131(4), 489-497. https://doi.org/10.1061/(ASCE)1090-0241(2005)131:4(489).

Danziger, F.A.B., Danziger, B.R., & Cavalcante, E.H. (2006). Discussion of "Review of standard penetration test short rod corrections" by Chris R. Daniel, John A. Howie, R. Scott Jackson, and Brian Walker. *Journal of Geotechnical and Geoenvironmental Engineering*, 132(12), 1634-1637. https://doi.org/10.1061/(ASCE)1090-0241(2006)132:12(1634).

Danziger, F.A.B., Danziger, B.R., & Cavalcante, E.H. (2008). Energy and the meaning of the N-value in SPT in special cases. In *Anais do 14° Congresso Brasileiro de Mecânica dos Solos e Engenharia Geotécnica (COBRAMSEG)* (pp. 2214-2224), Búzios, RJ (in Portuguese).

Décourt, L. (1982) Prediction of the bearing capacity of piles based exclusively on N values of the SPT. In *Proceedings of the 2nd European Symposium on Penetration testing – ESOPT II* (pp. 19-34), Amsterdam. https://doi.org/10.1201/9780203743959-4.

Décourt, L. (1989). General report/Discussion Session 2: SPT, CPT, pressuremeter testing and recent developments in in-situ testing – part 2: the standard penetration test, state-of-the-art report. In *Proceedings of the 12th International Conference on Soil Mechanics and Foundation Engineering* (Vol. 4, pp. 2405-2416), Rio de Janeiro, RJ.

Décourt, L., & Quaresma, A.R. (1978). Carga resistente de estacas a partir de valores de SPT. In *Anais do 6º Congresso Brasileiro de Mecânica dos Solos e Engenharia de Fundações (COBRAMSEF)* (Vol. 1, pp. 45-53). Rio de Janeiro: ABMS (in Portuguese).

Décourt, L., Muromachi, T., Nixon, I.K., Schmertmann, J.H., Thorburn, S., & Zolkov, E. (1988). Standard Penetration Test (SPT): international reference test procedure. In *Proceedings of the ISSMFE Technical Committee on Penetration Testing – SPT Working Party* (Vol. 1, pp. 3-26), Orlando.

Fairhurst, C. (1961). Wave mechanics of percussive drilling. *Mine & Quarry Engineering*, 27(3), 122-130.

Farrar, J.A., & Chitwood, D. (1999). CME *automatic hammer operations bulletin (report)*. Denver, CO: U.S. Department of Interior.

Gomes Correia, A., Viana da Fonseca, A., & Gambin, M. (2004). Routine and advanced analysis of mechanical in situ tests: results on saprolitic soils from granites more or less mixed in Portugal. In *Proceedings of the ISC-2 on Geotechnical and Geophysical Site Characterization* (Vol. 2, pp. 75-95). Rotterdam: Milpress.

Hachich, W., Villefort, L.F.C.B., & Schmidt, C.F. (2006). Comparison of SPT n-values obtained by manual and mechanized procedures. In *Anais do 13° Congresso Brasileiro de Mecânica dos Solos e Engenharia Geotécnica (COBRAMSEG)* (Vol. 2, pp. 613-618), Curitiba, Brasil (in Portuguese).

Hatanaka, M., & Uchida, A. (1996). Empirical correlation between penetration resistance and internal friction angle of sandy soils. *Soil and Foundation*, 36(4), 1-9. https://doi.org/10.3208/sandf.36.4_1.

Honeycutt, J.N., Kiser, S.E., & Anderson, J.B. (2014). Database evaluation of energy transfer for central mine equipment automatic hammer standard penetration tests. *Journal of Geotechnical and Geoenvironmental Engineering*, 140(1), 194-200. https://doi.org/10.1061/(ASCE)GT.1943-5606.0000988.

ISO 22476-3:2005+A1:2011. (2005). *Geotechnical investigation and testing – field testing – part 3: standard penetration test.* International Organization for Standardization, Geneva.

Ji, P., Yang, J., Zhang, N., Zhai, Q., Li, M., Wang, Y., Shen, T., & Satyanaga, A. (2023). Energy measurement in standard penetration tests. *Sustainability*, 15(6), 4763. http://dx.doi.org/10.3390/su15064763.

Johnsen, L.F., Bemben, S.M., & Jagello, J.J. (2001). SPT energy transfer measurements for liquefaction in the North-East. In *Proceedings of the International Conferences on Recent Advances in Geotechnical Earthquake Engineering and Soil Dynamics.* Missouri University of Science and Technology.

Kelley, S.P., & Lens, J.E. (2010). *Evaluation of SPT hammer energy variability* (Report No. 2010-3). Montpelier, VT: Vermont Agency of Transportation.

Kovacs, W.D. (1979). Velocity measurement of free-fall SPT hammer. *Journal of the Geotechnical Engineering Division*, 105(1), 1-10. https://doi.org/10.1061/AJGEB6.0000748.

Kovacs, W.D., & Salomone, L.A. (1984). Closure to "SPT Hammer Energy Measurement" by William D. Kovacs and Lawrence A. Salomone (April, 1982). *Journal of Geotechnical Engineering*, 110(4), 562-564. https://doi.org/10.1061/(ASCE)0733-9410(1984)110:4(562).

Kovacs, W.D., Salomone, L.A., & Yokel, F.Y. (1981). *Energy measurement in the standard penetration test.* Washington, D.C.: U.S. Department of Commerce.

Lee, C., An, S., & Lee, W. (2014). Real-time monitoring of SPT donut hammer motion and SPT energy transfer ratio using digital line-scan camera and pile driving analyzer. *Acta Geotechnica*, 9(6), 959-968. https://doi.org/10.1007/s11440-012-0197-0.

Lee, C., Lee, J.S., An, S., & Lee, W. (2010). Effect of secondary impacts on SPT rod energy and sampler penetration. *Journal of Geotechnical and Geoenvironmental Engineering*, 136(3), 522-526. http://dx.doi.org/10.1061/(ASCE)GT.1943-5606.0000236.

Lukiantchuki, J.A. (2012). *Interpretation of SPT test results based on dynamic instrumentation* [Doctoral thesis]. University of São Paulo (in Portuguese).

Lukiantchuki, J.A., Bernardes, G.P., & Esquivel, E.R. (2017). Energy ratio (E_R) for the standard penetration test based on measured field tests. *Soils and Rocks*, 40(2), 77-91. https://doi.org/10.28927/SR.402077.

Luza, M.E., Costa, G.A.S., Muguet, E.O., Cabral, F.S., & Danziger, F.A.B. (2024). Study of potential and kinetic energy in the SPT with a manually operated hammer. In *Anais do 21° Congresso Brasileiro de Mecânica dos Solos e Engenharia Geotécnica (COBRAMSEG*) (pp. 4460-4467), Balneário Camboriú, Brasil (in Portuguese). https://doi.org/10.47094/COBRAMSEG2024/540.

Mayne, P.W. (2001). Stress-strain-strength-flow parameters from enhanced in-situ tests. In *Proceedings of the International Conference on In-Situ Measurement of Soil Properties & Case Histories* (pp. 27-48), Bali, Indonesia.

Mello, V.F.B. (1971). The standard penetration test. In *Proceedings of the 4th Panamerican Conference on Soil Mechanics and Foundation Engineering* (Vol. 1, pp. 1-86), Porto Rico. ISSMGE.

Morgano, C.M., & Liang, R. (1992). Energy transfer in SPT: rod length effect. In *Proceedings of the 4th International Conference on the Application of Stress-Wave Theory to Piles* (pp. 121-127), Rotterdam.

Odebrecht, E. (2003). *SPT energy measurement* [Doctoral thesis]. Federal University of Rio Grande do Sul (in Portuguese).

Odebrecht, E., Schnaid, F., Rocha, M.M., & Bernardes, G.P. (2005). Energy efficiency for standard penetration tests. *Journal of Geotechnical and Geoenvironmental Engineering*, 131(10), 1252-1263. https://doi.org/10.1061/(ASCE)1090-0241(2005)131:10(1252).

CC BY

Ortiz, C., Alva, J., Oliden, J., Huarcaya, N., Riveros, G., & Raucana, R. (2025). Assessment of hammer energy measurement for the Standard Penetration Test (SPT) using pile driving analyzer and Kallpa analyzer devices in Peru. *Sensors*, 25(5), 1460. https://doi.org/10.3390/s25051460.

Palacios, A. (1977). *The theory and measurement of energy transfer during standard penetration test sampling* [Doctoral thesis]. University of Florida.

Palmer, D.J., & Stuart, J.G. (1957). Some observations on the Standard Penetration Test and a correlation of the test with a new penetrometer. In *Proceedings of the 4th International Conference on Soil Mechanics and Foundation Engineering* (pp. 231-236), London. ISSMGE.

Reading, P., Lovell, J., Spires, K., & Powell, J. (2010). The implications of the measurement of energy ratio (Er) for the standard penetration test. *Ground Engineering*, 43(5), 28-31.

Riggs, C.O., Mathes, G.M., & Rassieur, C.L. (1984). A field study of an automatic SPT hammer system. *Geotechnical Testing Journal*, 7(3), 158-163. https://doi.org/10.1520/GTJ10492J.

Sancio, R.B., & Bray, J.D. (2005). An assessment of the effect of rod length on SPT energy calculations based on measured field data. *Geotechnical Testing Journal*, 28(1), 22-30. https://doi.org/10.1520/GTJ11959.

Santana, C.M. (2015). *Instrumented SPT in calibration chamber* [Doctoral thesis]. COPPE, Federal University of Rio de Janeiro (in Portuguese).

Santana, C.M., Danziger, F.A.B., & Danziger, B.R. (2014). Energy measurement in Brazilian SPT system. *Soils and Rocks*, 37(3), 243-255. https://doi.org/10.28927/SR.373243.

Santana, C.M., Danziger, F.A.B., & Danziger, B.R. (2013). The measurement of Energy Reaching the Sampler in SPT. In *Proceedings of the 4th International Conference on Site Characterization* (Vol. 1, pp. 921-926), Porto de Galinhas.

Schmertmann, J.H., & Palacios, A. (1979). Energy dynamics of SPT. *Journal of the Geotechnical Engineering Division*, 105(8), 909-926. https://doi.org/10.1061/AJGEB6.0000839.

Schnaid, F., Odebrecht, E., Rocha, M.M., & Bernardes, G.P. (2009). Prediction of soil properties from the concepts of energy transfer in dynamic penetration tests. *Journal of Geotechnical and Geoenvironmental Engineering*, 135(8), 1092-1100. https://doi.org/10.1061/(ASCE)GT.1943-5606.0000059.

Seed, H.B., Tokimatsu, K., Harder, L.F., & Chung, R.M. (1985). Influence of SPT procedures in soil liquefaction resistance evaluations. *Journal of Geotechnical Engineering*, 111(12), 1425-1445. https://doi.org/10.1061/(ASCE)0733-9410(1985)111:12(1425).

Skempton, A.W. (1986). Standard penetration test procedures and the effects in sands of overburden pressure, relative density, particle size, ageing and overconsolidation. *Geotechnique*, 36(3), 425-447. https://doi.org/10.1680/geot.1986.36.3.425.

Srithar, S.T., & Ervin, M.C. (2001). Evaluation of the efficiency of an automatic SPT hammer. In *Proceedings of the International Conference on Soil Mechanics and Geotechnical Engineering* (pp. 511-514). ISSMGE.

Sy, A., & Campanella, R.G. (1991). An alternative method of measuring SPT energy. In *Proceedings of the 2nd International Conference on Recent Advances in Geotechnical Earthquake Engineering and Soil Dynamics* (pp. 499-505), St. Louis.

Yee, E., Stewart, J.P., & Tokimatsu, K. (2013). Elastic and large-strain nonlinear seismic site response from analysis of vertical array recordings. *Journal of Geotechnical and Geoenvironmental Engineering*, 139(10), 1789-1801. https://doi.org/10.1061/(ASCE)GT.1943-5606.0000900.

Yoshimi, Y., & Tokimatsu, K. (1983). SPT practice survey and comparative tests. *Soil and Foundation*, 23(3), 105-111. https://doi.org/10.3208/sandf1972.23.3_105.

Youd, T.L., Idriss, I.M., Andrus, R.D., Arango, I., Castro, G., Christian, J.T., Dobry, R., Finn, W.D.L., Harder, L.F., Hynes, M.E., Ishihara, K., Koester, J.P., Liao, S.S.C., Marcuson, W.F., Martin, G.R., Mitchell, J.K., Moriwaki, Y., Power, M.S., Robertson, P.K., & Stokoe, K.H. (2001). Liquefaction resistance of soils: summary report from the 1996 NCEER and 1998 NCEER/NSF workshops on evaluation of liquefaction resistance of soils. *Journal of Geotechnical and Geoenvironmental Engineering*, 127(10), 817-833. https://doi.org/10.1061/(ASCE)1090-0241(2001)127:10(817).